



## Metalorganic vapor-phase epitaxial growth of vertically well-aligned ZnO nanorods

W. I. Park, D. H. Kim, S.-W. Jung, and Gyu-Chul Yi

Citation: *Applied Physics Letters* **80**, 4232 (2002); doi: 10.1063/1.1482800

View online: <http://dx.doi.org/10.1063/1.1482800>

View Table of Contents: <http://scitation.aip.org/content/aip/journal/apl/80/22?ver=pdfcov>

Published by the [AIP Publishing](#)

---

### Articles you may be interested in

[Evidence for low density of nonradiative defects in ZnO nanowires grown by metal organic vapor-phase epitaxy](#)  
*Appl. Phys. Lett.* **91**, 143120 (2007); 10.1063/1.2794790

[Synthesis and optical properties of well-aligned ZnO nanorod array on an undoped ZnO film](#)  
*Appl. Phys. Lett.* **86**, 031909 (2005); 10.1063/1.1854737

[Optical and structural analysis of ZnCdO layers grown by metalorganic vapor-phase epitaxy](#)  
*Appl. Phys. Lett.* **83**, 3290 (2003); 10.1063/1.1620674

[Excitonic emissions observed in ZnO single crystal nanorods](#)  
*Appl. Phys. Lett.* **82**, 964 (2003); 10.1063/1.1544437

[Time-resolved and time-integrated photoluminescence in ZnO epilayers grown on Al<sub>2</sub>O<sub>3</sub> \(0001\) by metalorganic vapor phase epitaxy](#)  
*Appl. Phys. Lett.* **80**, 1924 (2002); 10.1063/1.1461051

---



# Metalorganic vapor-phase epitaxial growth of vertically well-aligned ZnO nanorods

W. I. Park, D. H. Kim, S.-W. Jung, and Gyu-Chul Yi<sup>a)</sup>

*Department of Materials Science and Engineering, Pohang University of Science and Technology (POSTECH), Pohang 790-784, Korea*

(Received 17 September 2001; accepted for publication 4 April 2002)

We report metalorganic vapor-phase epitaxial growth and structural and photoluminescent characteristics of ZnO nanorods. The nanorods were grown on  $\text{Al}_2\text{O}_3(00\cdot1)$  substrates at 400 °C without employing any metal catalysts usually needed in other methods. Electron microscopy revealed that nanorods with uniform distributions in their diameters, lengths, and densities were grown vertically from the substrates. The mean diameter of the nanorods is as narrow as 25 nm. In addition, x-ray diffraction measurements clearly show that ZnO nanorods were grown epitaxially with homogeneous in-plane alignment as well as a *c*-axis orientation. More importantly, from photoluminescence spectra of the nanorods strong and narrow excitonic emission and extremely weak deep level emission were observed, indicating that the nanorods are of high optical quality.

© 2002 American Institute of Physics. [DOI: 10.1063/1.1482800]

One-dimensional semiconductor nanowires and nanorods have attracted increasing interest due to their physical properties and diversity for potential electronic and photonic device applications.<sup>1,2</sup> Many nanowires including Si, Ge, InP, GaAs, GaN, and ZnO have been fabricated for applications since Si submicron whiskers were grown using a catalysis-assisted vapor-liquid-solid (VLS) growth method.<sup>3–5</sup> In VLS nanowire growth, impurities act as catalysts and play an essential role in forming liquid alloy droplets for deposition on a preferred site.<sup>5</sup> During growth, the catalyst might be incorporated into nanowires, and generate unintentional defect levels, e.g., Au used as a typical catalyst in VLS growth is well known to be a trap center in Si.<sup>6</sup> However, even low defect concentrations affect physical properties of semiconductors, and, hence, unintentionally doped impurities are detrimental to device fabrication. In this letter, we introduce metalorganic vapor-phase epitaxy (MOVPE) as a nanorod growth method which uses no metal catalyst.<sup>7</sup>

In addition to the control of impurities, heteroepitaxial growth and thickness control in the nanometer range are required for fabrication of sophisticated electronic and photonic devices. These are accomplished using advanced epitaxial growth techniques such as MOVPE and molecular beam epitaxy.<sup>8,9</sup> MOVPE is of particular interest since it has many advantages such as the feasibility of large area growth as well as simple and accurate doping and thickness control. Although this technique has widely been used for epitaxial film growth, it has rarely been employed for the preparation of one-dimensional nanorods.<sup>10</sup> In this letter, we report MOVPE growth of ZnO nanorods, which requires no metal catalysts. The nanorod growth temperature was as low as 400 °C. More importantly, nanorods grown in the course of this research are vertically well-aligned and exhibit uniform thickness and length distributions, which are very useful for many device applications.<sup>2,11</sup>

ZnO nanorods were grown on  $\text{Al}_2\text{O}_3(00\cdot1)$  substrates using a low pressure MOVPE system. For ZnO nanorod growth, diethylzinc (DEZn) and oxygen were employed as the reactants and argon was used as a carrier gas. Oxygen and DEZn flow rates were in the range of 20–100 and 0.5–5 sccm at a DEZn bubbler temperature of  $-15-0$  °C, respectively. A typical growth temperature was in the range of 400–500 °C.<sup>12,13</sup> Prior to ZnO nanorod growth, very thin ZnO buffer layers were grown at a low temperature. In this growth, no metal catalyst is coated on the substrates.

The crystal structure of ZnO nanorods was investigated by x-ray diffraction (XRD) including  $\theta-2\theta$  scan,  $\theta$ -rocking curve, and azimuthal ( $\phi$ ) scan measurements. The  $\theta$ -rocking curve and pole figure measurements were carried out for the (00·2) and (10·2) reflections of as-grown ZnO nanorods, respectively.

For optical characterization of the nanorods, photoluminescence (PL) spectroscopy was employed. The PL measurements were performed at room temperature with an optical resolution of 0.02–0.1 nm, and the 325 nm line of a continuous wave He–Cd laser was used as the excitation source. Details of the PL measurements have previously been reported.<sup>14</sup>

Field emission scanning electron microscopy (FE–SEM) clearly revealed the general morphology of the ZnO nanorods. As shown in Figs. 1(a) and 1(b), the images of ZnO nanorods grown for 1 h exhibited mean diameters and lengths of  $\sim 25$  and 800 nm, respectively. The diameter of nanorods obtained by MOVPE is somewhat smaller than the typical diameters of 50–100 nm for those prepared by other deposition methods.<sup>2,15,16</sup> Furthermore, the ZnO nanorods are well aligned vertically, showing uniformity in their diameters, lengths, and densities.

As shown in Fig. 1(c), hexagon-shaped pyramids were observed at the ends of MOVPE-grown ZnO nanorods. This observation suggests that the nanorods were grown by a non-catalysis growth mechanism. In the nanorod growth process using the catalysis-assisted VLS mechanism, nanosized

<sup>a)</sup>Author to whom correspondence should be addressed; electronic mail: gcyi@postech.ac.kr

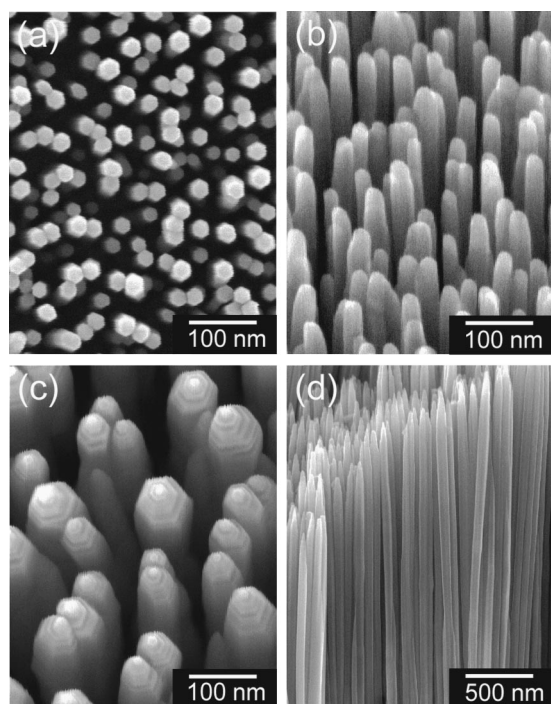


FIG. 1. FE-SEM (a) plan-view and (b) tilted images of ZnO nanorods with a mean diameter of  $\sim 25$  nm and (c) tilted and (d) cross-sectional images of ZnO nanorods with a mean diameter of  $\sim 70$  nm. In Fig. 1(c), hexagon-shaped pyramids with flat terraces and steps are shown at the ends of nanorods.

metal clusters have a critical role as a catalyst in forming liquid droplets that adsorb the gas-phase reactants where nanorod growth occurs. Hence, metallic nanoparticles are commonly observed at the end of nanorods grown by the catalysis-assisted VLS method.<sup>3–5,10,16</sup> For MOVPE-grown nanorods, however, flat terraces and steps on the hexagon-shaped ends are clearly shown in Fig. 1(c), which results from the layer-by-layer growth mode on the top layers of the nanorods. This is consistent with the previous report on similar hexagon-shape pyramids of microcrystalline grains in ZnO epilayers.<sup>17</sup> In addition, the ZnO nanorod tips were examined using energy dispersive x-ray (EDX) spectroscopy in the FE-SEM chamber, which confirmed that there was no metal clusters present. It is also noted that no impurity in the nanorods was observed within the detection limit of the EDX spectroscopy. These results exclude the possibility that the nanorods were grown by the catalysis-assisted growth mechanism.

The crystal structure and orientation of the as-grown nanorods were investigated measuring XRD. From the XRD  $\theta$ - $2\theta$  scan data of the ZnO nanorods [Fig. 2(a)] only two ZnO(00·2) and (00·4) peaks were observed at  $34.32^\circ$  and  $72.59^\circ$ , respectively. The observation of only (00· $l$ ) peaks indicates that nanorods were grown with a  $c$ -axis orientation. However, many ZnO nanorods prepared by other methods have been polycrystalline or grown with random orientations.<sup>15,16,18</sup> Meanwhile, XRD  $\theta$ -rocking curve measurements were also performed to investigate the degree of alignment to the normal direction of the surface. Figure 2(b) shows the rocking curve data of the sample shown in Fig. 1(a), indicating a full width at half maximum (FWHM) value of  $0.6^\circ$ . Typically, ZnO nanorods grown on  $\text{Al}_2\text{O}_3(00\cdot1)$

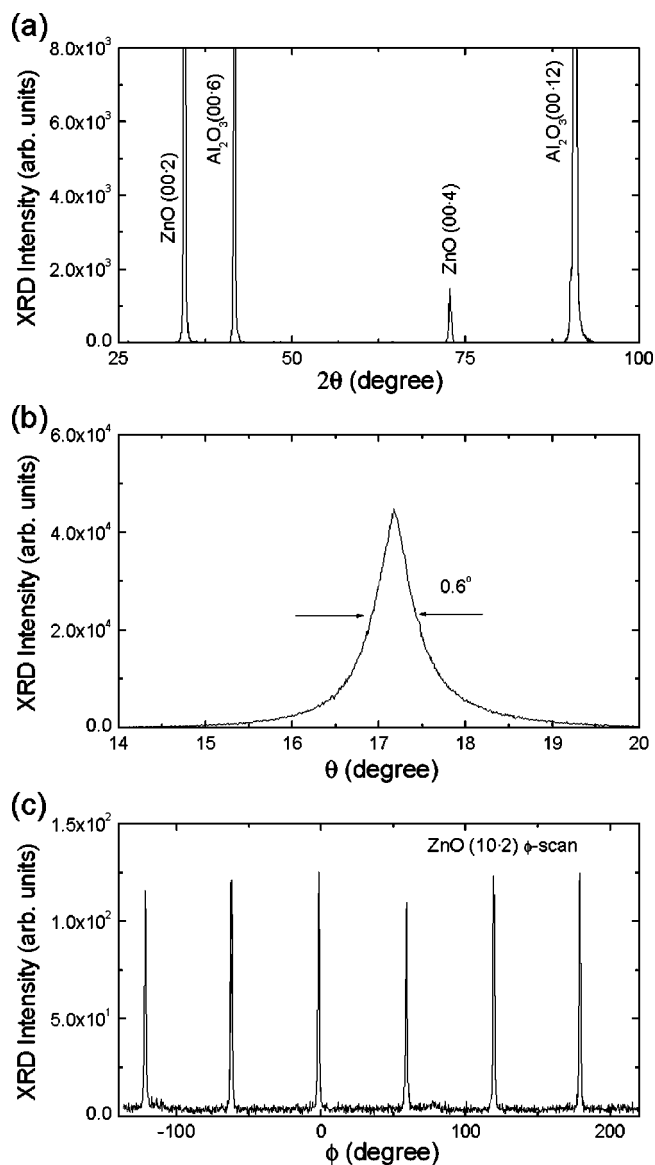


FIG. 2. XRD (a)  $\theta$ - $2\theta$  scan, (b) rocking curve, and (c) azimuthal ( $\phi$ ) scan measurement results of ZnO nanorods. From the XRD  $\theta$ - $2\theta$  scan data, only two peaks are shown at  $34.32^\circ$  and  $72.59^\circ$  which correspond to ZnO(00·2) and (00·4) peaks, respectively. The rocking curve also shows a FWHM value of  $0.6^\circ$ . A six-fold symmetry in  $\phi$ -scan data is also observed, indicating in-plane alignment of the nanorods.

substrates show a narrow FWHM in the range of  $0.1^\circ$ – $1^\circ$ , depending on the growth conditions. The narrow FWHM in the XRD rocking curves imply that the  $c$  axes of nanorods are well oriented along the normal direction of the substrate surface. Furthermore, Fig. 2(c) shows a six-fold rotational symmetry in the azimuthal scan. These results clearly indicate that the ZnO nanorods were epitaxially grown with homogeneous in-plane alignment as well as  $c$ -axis orientation. The in-plane alignment of nanorods is confirmed from the orientation of the facets in the FE-SEM image [Fig. 1(a)].

Figure 3 shows the FE-SEM images of ZnO nanorods at early stages of the nanorod growth. The nanorods exhibited the mean diameters of 13 and 16 nm after growth for 6 and 10 min, respectively. After further growth for 1 h, however, the nanorods exhibited only a little increase in the diameter but significant increase in the length. This result strongly suggests that the nanorods are grown on ZnO nuclei and the

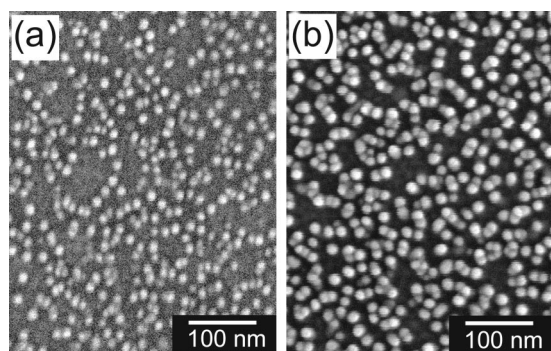


FIG. 3. FE-SEM images of ZnO nanorods grown for (a) 6 and (b) 10 min. The nanorods grown for 6 and 10 min show the mean diameter of 13 and 16 nm, respectively. Nanorods grown in this method show only a little increase in the diameters with increasing growth time.

nanorod formation results from the higher growth rate along the  $c$ -axis direction. However, it is noted that the spacing of the nanorods becomes larger with increasing growth time, which might result from a “crowding effect” of closely spaced that strongly favors upward growth.

As for the mechanism of the nanorod growth, nucleation at the initial stage might have a crucial role in both the vertical and in-plane alignments of the nanorods. Since the metal catalyst is not used for the nanorod growth in this research, the nucleation can occur at any sites on the substrate. During the formation of nuclei, ZnO nuclei are grown with an epitaxial relationship with  $\text{Al}_2\text{O}_3(00\cdot 1)$  since ZnO and  $\text{Al}_2\text{O}_3$  are lattice matched.<sup>12</sup> This argument is strongly supported by the fact that FWHM values in XRD rocking curves of the nanorods were decreased by the use of low temperature ZnO buffer layer, presumably due to enhanced epitaxy of ZnO nuclei.

The optical properties of the ZnO nanorods were investigated by PL spectroscopy. From room temperature PL spectrum of ZnO nanorods in Fig. 4, the dominant peak was observed at 3.29 eV, which is attributed to the free exciton peak.<sup>12–14</sup> The FWHM of the free exciton peak was as narrow as 90 meV. This result indicates that a PL peak shift due to the quantum confinement effect is not observed in these ZnO nanorods, presumably due to the large diameters of nanorods exceeding 20 nm. Meanwhile, the deep level green emission associated with point defects commonly observed in ZnO epilayers was found to be extremely weak compared with the near band edge emission. The weak deep level emission might be related to the low impurity concentration determined by EDX spectroscopy. The strong and sharp excitonic emission and low deep level emission indicate that the ZnO nanorods are of excellent optical quality, comparable to the ZnO epilayers.

In conclusion, MOVPE demonstrated the epitaxial growth of vertically aligned ZnO nanorods at a low temperature of 400 °C. In this process, no metal catalyst was used. The FE-SEM images showed uniform thickness and length distributions. Furthermore, the nanorods are of high crystal-

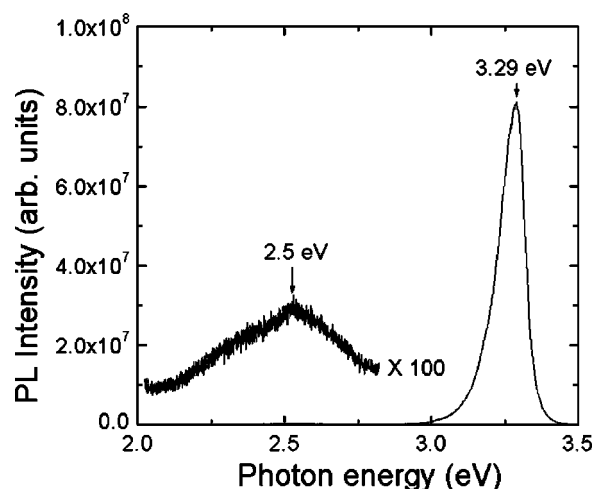


FIG. 4. PL spectrum of ZnO nanorods measured at room temperature. A dominant free exciton peak at room temperature was observed at 3.29 eV, indicating no peak shift due to the quantum confinement. Deep level emission is also shown to be extremely weak even at room temperature.

linity and excellent optical quality. XRD measurements exhibited both in-plane aligned and  $c$ -axis oriented growth of nanorods. From the PL spectra measured at room temperature, a narrow and strong emission peak was observed at 3.29 eV with a very weak deep level emission.

This work was supported by the KOSEF through the Regional University Research Program. Extensive use of the facilities at POSTECH is acknowledged.

- <sup>1</sup>X. Duan, Y. Huang, Y. Cui, J. Wang, and C. M. Lieber, *Nature (London)* **409**, 66 (2001).
- <sup>2</sup>M. H. Huang, S. Mao, H. Feick, H. Yan, Y. Wu, H. Kind, E. Weber, R. Russo, and P. Yang, *Science* **292**, 1897 (2001).
- <sup>3</sup>X. Duan and C. M. Lieber, *Adv. Mater.* **12**, 298 (2000).
- <sup>4</sup>J. Hu, T. W. Odom, and C. M. Lieber, *Acc. Chem. Res.* **32**, 435 (1999).
- <sup>5</sup>R. S. Wagner and W. C. Ellis, *Appl. Phys. Lett.* **4**, 89 (1964).
- <sup>6</sup>S. Braun and H. G. Grimmeiss, *J. Appl. Phys.* **45**, 2658 (1974).
- <sup>7</sup>M. He, I. Minus, P. Zhou, S. N. Mohammed, J. B. Halpern, R. Jacobs, W. L. Sarney, L. Salamanca-Riba, and R. D. Vispute, *Appl. Phys. Lett.* **77**, 3731 (2000).
- <sup>8</sup>G. B. Stringfellow, *Organometallic Vapor-Phase Epitaxy: Theory and Practice* (Academic, Boston, 1989).
- <sup>9</sup>A. Y. Cho and I. Hayashi, *J. Appl. Phys.* **42**, 4422 (1971).
- <sup>10</sup>M. Yazawa, M. Koguchi, A. Muto, M. Ozawa, and K. Hiruma, *Appl. Phys. Lett.* **61**, 2051 (1992).
- <sup>11</sup>S. Fan, M. G. Chapline, N. R. Franklin, T. W. Tomblor, A. M. Cassell, and H. Dai, *Science* **283**, 512 (1999).
- <sup>12</sup>W. I. Park, S.-J. An, G.-C. Yi, and H. M. Jang, *J. Mater. Res.* **16**, 1358 (2001).
- <sup>13</sup>W. I. Park, G.-C. Yi, and H. M. Jang, *Appl. Phys. Lett.* **79**, 2022 (2001).
- <sup>14</sup>W. I. Park and G.-C. Yi, *J. Electron. Mater.* **30**, L32 (2001).
- <sup>15</sup>Y. C. Kong, D. P. Yu, B. Zhang, W. Fang, and S. Q. Feng, *Appl. Phys. Lett.* **78**, 407 (2001).
- <sup>16</sup>M. H. Huang, Y. Wu, H. Feick, N. Tran, E. Weber, and P. Yang, *Adv. Mater.* **13**, 113 (2001).
- <sup>17</sup>Z. K. Tang, G. K. L. Wong, P. Yu, M. Kawasaki, A. Ohtomo, H. Koinuma, and Y. Segawa, *Appl. Phys. Lett.* **72**, 3270 (1998); M. Kawasaki, A. Ohtomo, I. Ohkubo, H. Koinuma, Z. K. Tang, P. Yu, G. K. L. Wong, B. P. Zhang, and Y. Segawa, *Mater. Sci. Eng., B* **56**, 239 (1998).
- <sup>18</sup>Y. Li, G. W. Meng, L. D. Zhang, and F. Phillipp, *Appl. Phys. Lett.* **76**, 2011 (2000).